

Mechanical Properties of Strontium Ferrites with Duplex Structure

Takanori Watari,^a Hironobu Hyakutake,^a Toshio Torikai,^a Ohsaku Matsuda,^a
Masaji Endo^b & Takahiro Motone^b

^a Department of Applied Chemistry, Faculty of Science and Engineering, Saga University, 1 Honjo, Saga 840, Japan

^b Kyusyu Sumitoku Electronics Co. Ltd, 282 Fukumo, Ohmachi, Kishimagun, Saga 849-21, Japan

(Received 20 December 1993; accepted 6 June 1994)

Abstract: The microstructures and the mechanical properties of the strontium ferrites (Sr-ferrites) with duplex structure were examined. As-received Sr-ferrites had a homogeneous microstructure and their average grain size was 1.58 μm . Some grains increased up to 106 μm and 228 μm in size after annealing at 1250°C for 1 h and 6 h, respectively. The volume fractions of the large grains were 4% after 1 h-annealing and 45% after 6 h-annealing. According to the microstructural evolution, the bending strength decreased from 148 MPa (as-received) to 140 MPa (3 h-annealing) and 93 MPa (6 h-annealing), but the fracture toughness increased from 2.14 MPa $\cdot\text{m}^{1/2}$ (as-received) to 2.20 MPa $\cdot\text{m}^{1/2}$ (3 h-annealing) and 2.36 MPa $\cdot\text{m}^{1/2}$ (6 h-annealing). These results indicated that the large grains in the duplex structure acted as both fracture origins and reinforcements. The Weibull modulus of materials was improved from 7 (as-received materials) to 17 (material after 3 h-annealing) and 9.5 (material after 6 h-annealing).

1 INTRODUCTION

Microstructural designing of ceramics has been widely investigated to improve the fracture toughness (K_{IC}) and the Weibull modulus (m) of engineering ceramics.^{1,2} One effective design is to incorporate ceramic fibers, whiskers or platelets with a high aspect ratio into ceramics. For example, by the incorporation of SiC whisker (20 vol%) to alumina, K_{IC} of the specimen increased from ~ 3 MPa $\cdot\text{m}^{1/2}$ to ~ 9 MPa $\cdot\text{m}^{1/2}$ and the m -value also increased from 4.6 to 13.4.¹

There are various methods of fabricating the reinforced ceramic composites. One is the sintering of the powder compact mixed with the reinforcements as mentioned before. However, it is very difficult to densify such a compact by common pressureless sintering.^{3–5} Hot isostatic pressing is necessary to obtain dense composites. However, this process leads to high cost. Another method is the *in situ* formation of grains with anisotropic shapes in a ceramic matrix. Okada *et al.*⁶ com-

pared the K_{IC} of yttria-doped zirconia/mullite composites prepared by three processes: *in situ* whisker growth (IS), physical mixing of ZrO₂ powders and mullite whiskers (PM), and reaction sintering (RS). They showed the superiority of the *in situ* process to improve the fracture toughness, for example K_{IC} of each composite was 8 MPa $\cdot\text{m}^{1/2}$ (RS), 12.8 MPa $\cdot\text{m}^{1/2}$ (PM), and 15 MPa $\cdot\text{m}^{1/2}$ (IS) for ZrO₂/mullite (15wt%) composites.

Strontium hexaferrite (SrFe₁₂O₁₉, Sr-ferrite) is one of the well-known materials for permanent magnets.⁷ The magnetic and mechanical properties of sintered Sr-ferrites depend on its microstructure. In order to fabricate a sintered magnet with superior properties, it is necessary to inhibit the grain growth during sintering, and also to keep the microstructure homogeneous. For this reason, some oxides are added to the Sr-ferrites. However, in spite of, or because of, these additives, the exaggerated grain growth or secondary recrystallization has been observed in the ferrite magnets.⁸

The exaggerated large grains of Sr-ferrites usually have platelet shape. The microstructure, in which some large grains coexist with many small grains, is called a duplex structure. The process developing this duplex structure is one of the *in situ* processes and the resulting product is regarded as a material self-reinforced by platelet grains. However, there are few reports with this point of view. The present study was conducted, focusing on the mechanical properties of the sintered Sr-ferrites with duplex structures.

2 EXPERIMENTAL PROCEDURE

2.1 Sample preparation

Sr-ferrite materials were supplied from Kyusyu Sumitoku Electronics Co., Ltd. The outline of the fabrication process was as follows; the mixture of SrCO_3 and Fe_2O_3 powders was calcined at 1300°C to form $\text{SrFe}_{12}\text{O}_{19}$. The obtained Sr-ferrite was then crushed into fine powders under $1\mu\text{m}$ in diameter, and mixed with a large amount of water and some additives. This slurry was poured into a die and pressed under a magnetic field. Next, the green body was sintered at 1230°C for one hour in air. The composition of the obtained Sr-ferrite is listed in Table 1. The as-received materials were annealed at 1250°C for 1, 3, 6 and 10 h in air to develop duplex structures.

2.2 Analysis

The samples were polished with SiC powders and then diamond powders for measurement of the mechanical properties and observation of microstructures.

The three-point bending test was performed using a specimen of $4 \times 3 \times 40$ mm based on JIS-R1601 (Japan Industrial Standards-R1601). The span length was 30 mm and the crosshead speed was 0.5 mm/min. The fracture toughness was evaluated, based on the measurement method reported by Yasuda *et al.*⁹ using a specimen of $4 \times 3 \times 20$ mm with a chevron notch. A 15 mm-span and crosshead speed of 0.005 mm/min were adopted.

After the bending test, the polished surface of the specimen was etched in an acid solution con-

taining $\text{HF}:\text{HNO}_3 = 1:3$ at 110°C . The etched surface was observed with a metallurgical microscope. The grain size measurement was performed in two ways; the small grain size was measured by the linear intercept method¹⁰ and the large grain size was directly measured from the microscopic photographs. The volume fraction ratio of large to small grains was evaluated by quantitative stereology (point count method)¹⁰ using the photographs for the etched surface.

The orientation degree was calculated by means of Lotgering's method¹¹ using an X-ray diffraction (XRD) pattern of Sr-ferrite body. The XRD pattern was measured parallel to the magnetic field direction in a molding process. The density was measured by the Archimedes method. The magnetic properties were measured with a B-H tracer using the same specimens as used in the bending test.

3 RESULTS AND DISCUSSION

3.1 Microstructure

Although the Sr-ferrite particles had irregular shapes, each grain of sintered bodies was a platelet as shown in Fig. 1 (a) and (b). The symbols // and \perp in the photograph denote parallel and perpendicular to the direction of the magnetic field applied on molding compacts, respectively. The plane of each platelet was almost oriented perpendicular to the magnetic field direction. This orientation of the platelet grains could be explained by the following reasoning. The magnetic field rotated each Sr-ferrite particle to orient its hexagonal axis (*c*-axis) parallel to the magnetic field direction because the *c*-axis is a preferred direction of the magnetization. The orientation degree of (00 l) plane showed a high value of 0.72 for as-received material. During the annealing, the crystal plane of grains preferentially grew perpendicular to the *c*-axis, and the large platelets as shown in Fig. 1 were formed.¹² Hereafter, the average length and width of the platelet grains were denoted *la* and *lw*, respectively. In the as-received sample, *la* and *lw* were 1.58 μm and 1.13 μm , respectively, and the aspect ratio (*la/lw*) was about 1.4. The microstructures of the specimen annealed at 1250°C for 6 h are shown in Fig. 1 (c)–(f). Some of the grains grew more rapidly than others, forming a duplex structure. Due to this grain growth, pores were trapped in the large grain [Fig. 1 (c)]. The large grains were hexagonal [Fig. 1 (e)].

The duplex structure changed with increasing annealing time as shown in Fig. 2. The number in the picture indicates the volume fraction (V_f) of

Table 1. Chemical composition of the Sr-ferrite

Chemical composition Content (wt%)	Fe_2O_3	SrO	CaO	SiO_2	Al_2O_3
	86.54	9.24	0.68	0.65	0.45

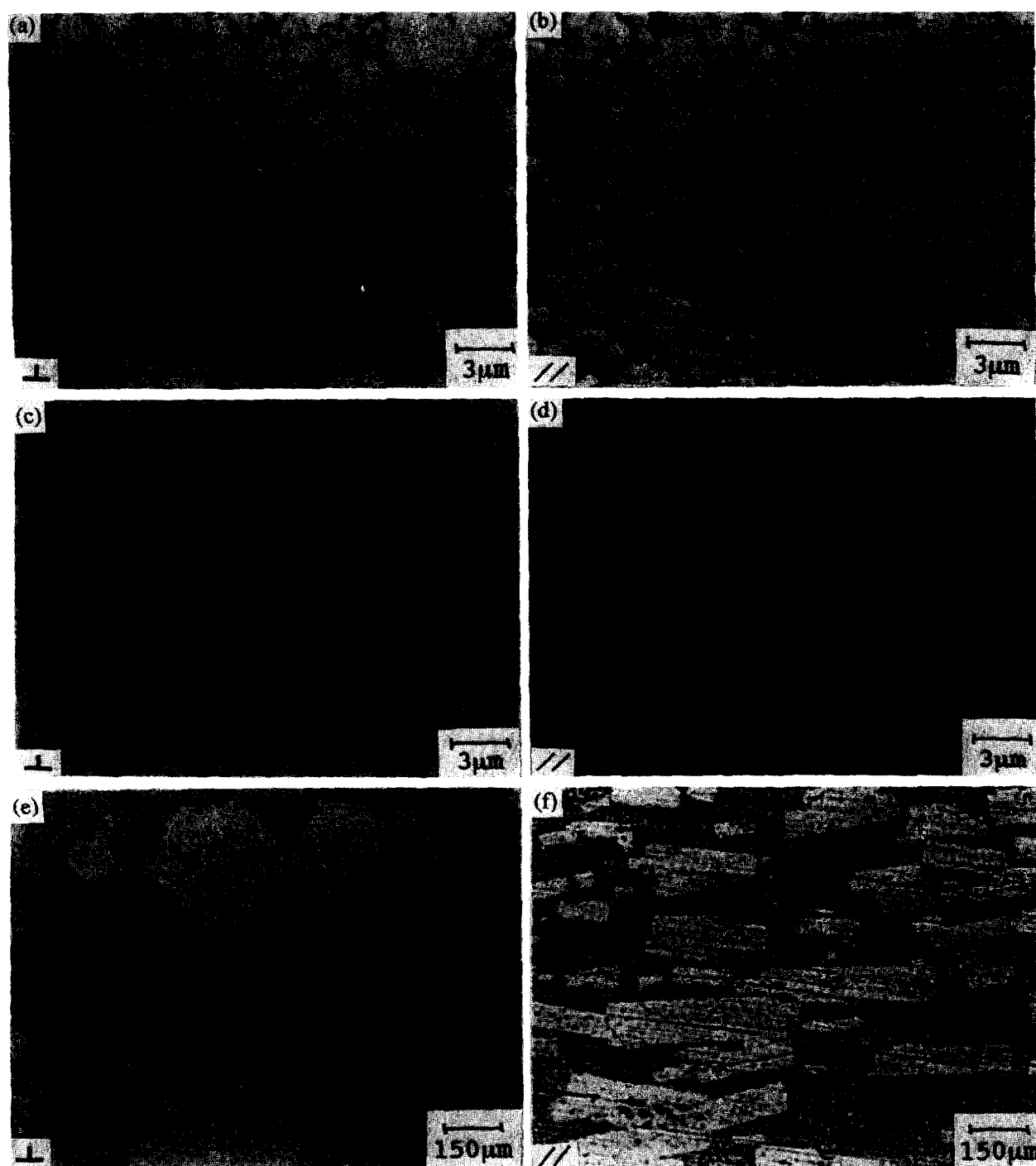


Fig. 1. Microstructure of the Sr-ferrites. (a) and (b): as received; (c)–(f): annealed at 1250°C for 6 h.

the large grains. Both the grain size (l_a) and V_f of the large grains increased with increasing time. In particular, V_f and the number of the large grains abruptly increased during annealing between 3 h and 6 h. The grains with intermediate size could not be observed. The grain sizes (l_a , l_w) of the large grains and l_a of the small grains are shown in Fig. 3. The numbers in Fig. 3 indicate the orientation degree of (00 l) plane. The grain size of Sr-ferrites annealed for 10 h could not be measured because the grain boundaries between large grains were not clear and distinguished as shown in Fig. 2 (d). Also, in this sample, some cracks

could be seen in large grains. The cracks might be caused by thermal expansion anisotropy of Sr-ferrite crystal (thermal expansion coefficient for // c -axis = $14 \times 10^{-6}/\text{K}$, and $\perp c$ -axis = $10 \times 10^{-6}/\text{K}$).⁷ The orientation degree in this sample was 0.87. The large grains grew up to 106 μm after 3 h-annealing, but the small grains grew up to just 1.9 μm . With increasing annealing time, the small grains hardly grew, but the large grains grew up to 228 μm for 6 h, keeping l_w almost constant ($\sim 50 \mu\text{m}$). Therefore, the aspect ratio of the large grains increased from 1.4 (0 h) to 1.5 (1 h), 2.5 (3 h), and 3.1 (6 h). The degree of orientation

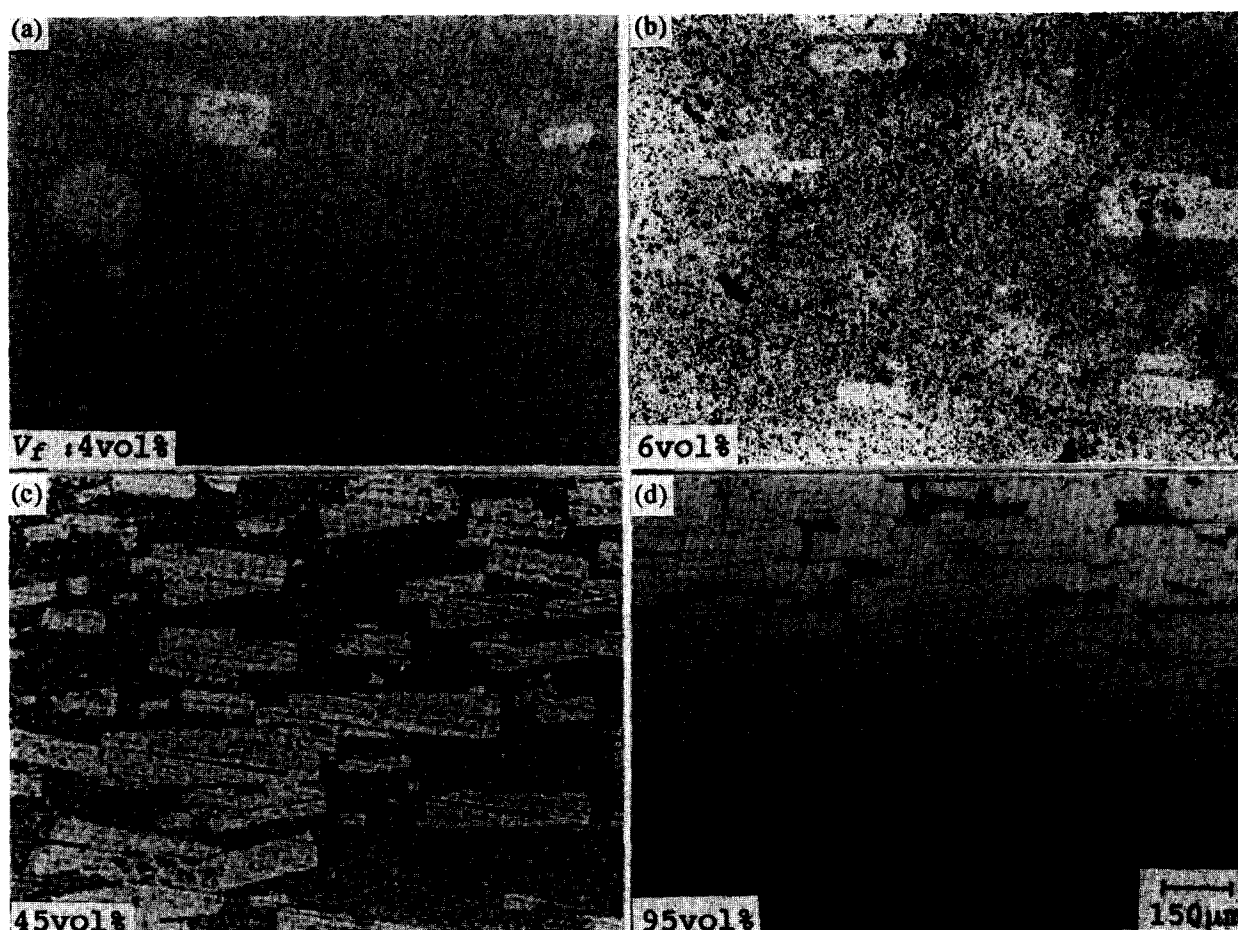


Fig. 2. Microstructural evolution of the Sr-ferrites after annealing at 1250°C for (a) 1 h; (b) 3 h; (c) 6 h; (d) 10 h.

increased during annealing between 3 h and 6 h and, at the same time, V_f increased as mentioned before. These phenomena were explained by Stuijts,¹³ who reported that the crystals incorrectly aligned were eliminated to decrease the boundary energy between the crystals.

3.2 Mechanical properties

The average bending strength of as-received and annealed Sr-ferrites were obtained using 20 specimens. The measurement was performed parallel to

the magnetic field on molding compacts, i.e. perpendicular to the platelet plane. On calculating the average strength, the specimens with some large pores as shown in Fig. 1 (e) were excluded. The anisotropy in strength of ferrite magnets were discussed in other papers.¹⁴⁻¹⁶ The relation between the average bending strength and the annealing time is shown in Fig. 4. The strength of as-received sample was 148 MPa. This value is almost the same as those reported by Hamamura¹⁴ and With¹⁵. The strength of the annealed sample decreased with annealing time. In particular, the degradation of the strength occurred remarkably

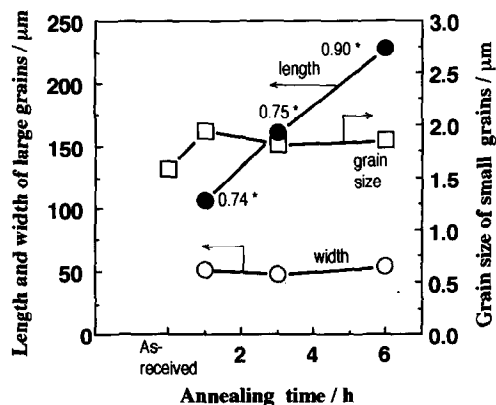


Fig. 3. Length (●) and width (○) of large grains, grain size (□) of small grains of the Sr-ferrites as a function of annealing time. * denotes the orientation degree of (00*l*) plane.

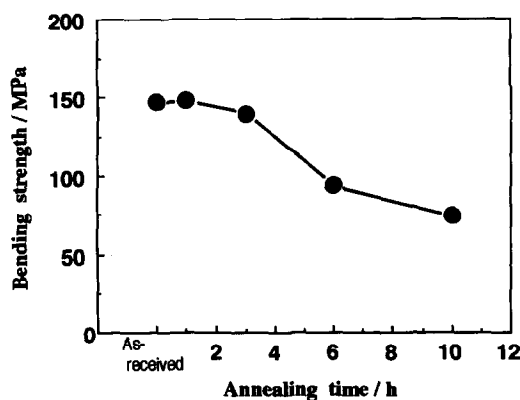


Fig. 4. Bending strength of the Sr-ferrites as a function of annealing time.

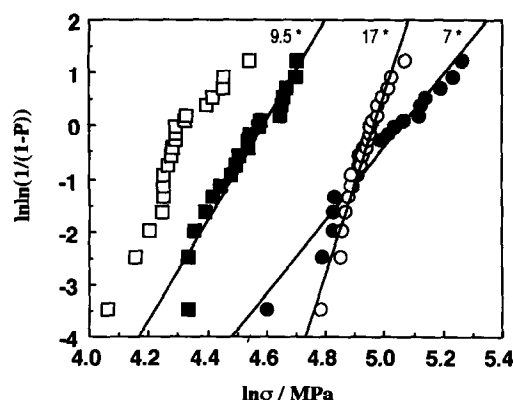


Fig. 5. Weibull plots on as-received and annealed Sr-ferrites (P ; probability of failure. σ , bending strength). Annealing time: (●) 0 h, (○) 3 h, (■) 6 h, and (□) 10 h. * denotes the Weibull moduli.

after annealing between 3 h and 6 h. Usually, the strength of sintered ceramics depend on their microstructure, for example, porosity, pore size, grain size and inclusions.¹⁷ In the present study, the porosity of Sr-ferrites was almost constant (5–6 vol%) with annealing time. The pores at grain boundaries were 0.1–2 μm in size and the pores incorporated in the large grains were 1–2 μm in size, as shown in Fig. 1 (c) and (d). The sizes of these pores are much smaller than those of the large grains, and the contents of large grains drastically increased after annealing between 3 h and 6 h as shown in Fig. 2. These results indicate that the large grain acted as the fracture origin in the Sr-ferrites with a duplex structure like the inclusion embedded in ceramic body.

The Weibull plots of each sample are shown in Fig. 5. The Weibull moduli (m) obtained from the slope of each line are indicated in the figure. The m -value of as-received specimen was 7 and this value was almost the same as that of Mg–Mn–Zn ferrite.¹⁸ The m -value of the sample annealed for 3 h was 17 and this value was almost the same as those of engineering ceramics.¹⁹ The Weibull plots of the specimen annealed for 10 h

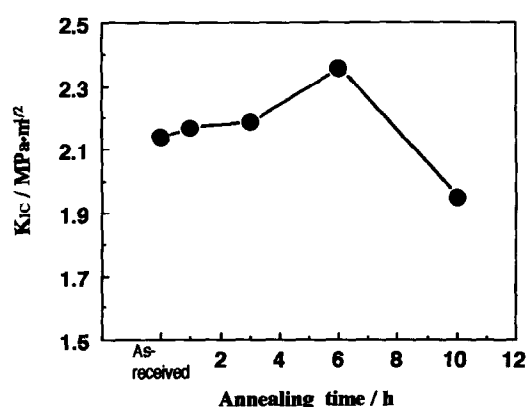


Fig. 6. Fracture toughness of the Sr-ferrites as a function of annealing time.

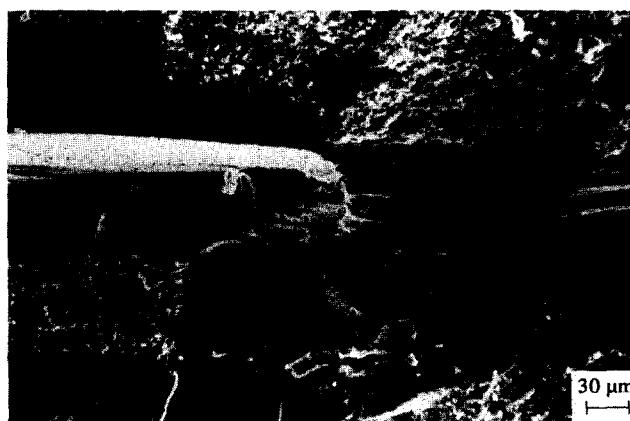


Fig. 7. Fracture surface of the Sr-ferrite annealed at 1250°C for 6 h.

seems to be represented by two straight lines. This may be due to the difference of the fracture origins, for example, large grains, cracks (Fig. 2), and an internal stress, in the specimen.

The relation between fracture toughness (K_{IC}) and annealing time is shown in Fig. 6. K_{IC} increased from 2.14 $\text{MPa}\cdot\text{m}^{1/2}$ to 2.36 $\text{MPa}\cdot\text{m}^{1/2}$ with increasing annealing time from 0 h to 6 h. This behavior is just the opposite of that observed in the bending strength. However, the increment of K_{IC} was very small compared with those of platelet reinforced composites previously mentioned. For example, Chen and Chen²⁰ prepared the composites consisting of alumina/aluminate platelet using an *in situ* process and reported that the fracture toughness increased from 3.0 $\text{MPa}\cdot\text{m}^{1/2}$ to 4.3 $\text{MPa}\cdot\text{m}^{1/2}$ by incorporation of aluminate platelets. Also, Claaßen and Claussen²¹ reported that the incorporation of SiC platelet increased K_{IC} value of alumina from 4.2 $\text{MPa}\cdot\text{m}^{1/2}$ to 6.8 $\text{MPa}\cdot\text{m}^{1/2}$. In these platelet-reinforced ceramics, toughening mechanism such as debonding, bridging, and pull-out could be available.²² However, in order to use these mechanisms effectively, the platelet size should be small (5–20 μm), the volume fraction of

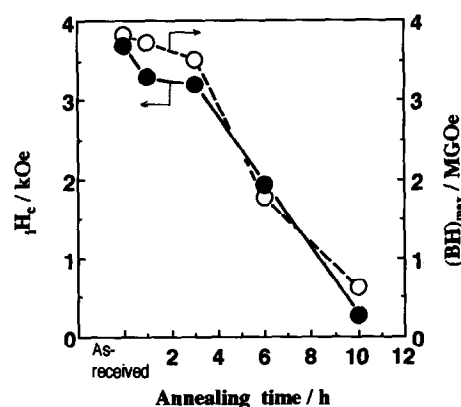


Fig. 8. Magnetic properties of the Sr-ferrites after annealing: (●) H_c and (○) $(BH)_{\text{max}}$.

the platelet should be optimum (i.e. 15–20 vol% for alumina/silicon carbide platelet composite) and the interface bonding strength between platelet and matrix should be optimum. In the present study, however, the grains grew up to 110–230 μm and the volume fraction of the large grains could not be controlled easily. Figure 7 shows the fracture surface of Sr-ferrite annealed at 1250°C for 6 h. This picture shows the trace of debonding of the platelet, but the main fracture was transgranular. The bridging and pull-out of the platelet grains did not appear. This might be due to larger platelets and the strong interface bonding between platelet and matrix. More careful heat-treatment and selection of any other additives are necessary to control the microstructure and the interface bonding strength, and to improve the fracture toughness of Sr-ferrite with duplex structure, keeping the bending strength constant.

3.3 Magnetic properties

The magnetic remanence, B_r , of the Sr-ferrite magnet depends on its relative density and the orientation degree of (00 l) plane, but independent on the grain size.²³ In the present study, the relative density of the samples were constant (94–95%) and the orientation degree was very high (0.72–0.90) as mentioned above. Therefore, B_r of all the specimens were almost constant, about 0.4 T. On the other hand, the magnetic coercivity, H_c , and the maximum energy product, $(BH)_{\text{max}}$, decreased with increasing annealing time, that is, with increasing grain size as shown in Fig. 8. The magnetic domain in the large Sr-ferrite grain was easily divided into many regions with opposite orientation of the magnetization under the opposite magnetic field. This domain structure decreased H_c and $(BH)_{\text{max}}$.

4 CONCLUSIONS

The *in situ* process using secondary recrystallization was examined to improve the fracture toughness of Sr-ferrites. The results are summarized as follows:

- (1) Sr-ferrites, in which small grains coexisted with large platelet grains, could be obtained by making use of an anisotropic grain growth.
- (2) The large platelet grains increased the fracture toughness of the Sr-ferrite with duplex structure by acting as reinforcements, but decreased the bending strength by acting as fracture origin.

- (3) Introducing duplex structure into Sr-ferrites increased the Weibull modulus of materials.

ACKNOWLEDGEMENTS

The authors are sincerely grateful to Mr Shiwa and Mr Takigawa of Kyusyu Sumitoku Electronics Company Co., Ltd for supply of Sr-ferrites, and to Mr Ichinose of Saga Ceramic Research Laboratory for preparing test samples.

REFERENCES

1. BECHER, P. F., Microstructural design of toughened ceramics. *J. Am. Ceram. Soc.*, **74** (1991) 255–69.
2. HARMER, M. P., CHAN, H. M. & MILLER, G. A., Unique opportunities for microstructural engineering with duplex and laminar ceramic composites. *J. Am. Ceram. Soc.*, **75** (1992) 1715–28.
3. TIEGS, T. N. & BECHER, P. F., Sintered Al_2O_3 -SiC-whisker composites. *Am. Ceram. Soc. Bull.*, **66** (1987) 339–42.
4. WEISER, M. W. & JONGHE, L. C., Inclusion size and sintering of composite powders. *J. Am. Ceram. Soc.*, **71** (1988) C-125–C-127.
5. LEE, H. & SACKS, M. D., Pressureless sintering of SiC-whisker-reinforced Al_2O_3 composites: I. Effect of matrix powder surface area. *J. A. Ceram. Soc.*, **73** (1990) 1884–93.
6. OKADA, K., OTSUKA, N., BROOK, R. J. & MOULSON, A. J., Microstructure and fracture toughness of yttria-doped tetragonal zirconia polycrystal/mullite composites prepared by an *in situ* method. *J. Am. Ceram. Soc.*, **72** (1989) 2369–72.
7. STÄBLEIN, H., Hard ferrites and plastroferrites. In *Ferromagnetic materials*, Vol. 3, ed. E. P. Wohlfarth, North-Holland, Amsterdam, 1982, pp. 441–602.
8. KINGERY, W. D., BOWEN, H. K. & UHLMANN, D. R., *Introduction to Ceramics*, 2nd edn. John Wiley, New York, 1976, pp. 461–8.
9. YASUDA, E., AKATSU, T. & TANABE, Y., Influence of whiskers' shape and size on mechanical properties of SiC whisker-reinforced Al_2O_3 . *J. Jap. Ceram. Soc.*, **99** (1991) 52–8.
10. UNDERWOOD, E. E., COLCORD, A. R., & WAUGH, R. C., Quantitative relationships for random microstructures. In *Ceramic Microstructures*, ed. R. M. Fulrath & J. A. Pask, Robert E. Krieger Publishing, New York, 1976, pp. 25–52.
11. LOTGERING, F. K., *J. Inorg. Nucl. Chem.*, **9** (1959) 113–23.
12. STUIJTS A. L., RATHENAU G. W. & WEBER G. H., Ferroxidure II and III, Anisotropic permanent magnet materials. *Philips Tech. Rev.*, **16** (1954) 141–7.
13. STUIJTS, A. L., Sintering of ceramic permanent magnetic material. *Trans. Brit. Ceram. Soc.*, **55** (1956) 57–74.
14. HAMAMURA, A., The mechanical strength of ferrite magnet and its application. *Sumitomo Tokusyu Kinzoku Giho*, **1** (1973) 37–46. (Japanese)
15. WITH, G., Anisotropy in mechanical properties of sintered Sr-hexaferrite. *Silic. Ind.*, **49** (1984) 185–9.
16. IWASA, M., LIANG, E. C., BRADT, R. C. & NAKAMURA, Y., Fracture of isotropic and textured Ba hexaferrite. *J. Am. Ceram. Soc.*, **64** (1981) 390–3.
17. *Seramikku Sentan Zairyo-kyodo to Bikouzou*, pp. 218–59. Japanese Ceramic Society, Japan, 1991.
18. OVRI, J. E. & DAVIES, T. J., Uniaxial and biaxial strengths of a sintered ferrite. In *Science of Ceramics*,

- Vol. 14, ed. D. Tayler, The Institute of Ceramics, Stoke on Trent, 1988, pp. 599–605.
19. RICE, R. W., Toughening in ceramic particulate and whisker composites. *Ceram. Eng. Sci. Proc.*, **11** (1990) 667–94.
20. CHEN, P. & CHEN, I., *In situ* alumina/aluminate platelet composites. *J. Am. Ceram. Soc.*, **75** (1992) 2610–12.
21. CLAABEN, T. & CLAUSSEN, N., Processing of ceramic-matrix/platelet composites by tape casting and lamination. *J. Eur. Ceram. Soc.*, **10** (1992) 263–71.
22. CLAUSSEN, N., Ceramic platelet composites. In *Structural Ceramics—Processing, Microstructure and Properties*, ed. J. J. Bentze, Risø National Laboratory, Roskilde, 1990, pp. 1–12.
23. OJIMA, T., Hard ferrite material (Japanese). In *Ferrite*, ed. T. Hiraga, K. Okutani & T. Ojima, Maruzen, 1986, pp. 125–50.